MEDICAL SCIENCE MONITOR

LAB/IN VITRO RESEARCH

e-ISSN 1643-3750
© Med Sci Monit, 2019; 25: 4094-4103
DOI: 10.12659/MSM.914202

Received: 2018.11.20
Accepted: 2019.02.08
Published: 2019.06.02

miR-466 and NUS1 Regulate the AKT/Nuclear Factor kappa B (NFκB) Signaling Pathway in Intrauterine Adhesions in a Rat Model

Authors' Contribution:
Study Design A
Data Collection B
Statistical Analysis C
Data Interpretation D
Manuscript Preparation E
Literature Search F
Funds Collection G

AC 1 Min Liu*
BDE 2 Dapeng Zhao*
CDE 3 Xingguo Wu*
BF 4 Song Guo
BD 4 Li Yan
CD 4 Shan Zhao
BE 3 Hua Li
CDEG 3 Yongmei Wang
AG 4 Fengnian Rong

1 School of Medicine, Shandong University, Jinan, Shandong, P.R. China
2 Department of Neurology, Taian City Central Hospital, Taian, Shandong, P.R. China
3 Department of Obstetrics and Gynecology, Taian City Central Hospital, Taian, Shandong, P.R. China
4 Department of Obstetrics and Gynecology, Affiliated Qianfoshan Hospital of Shandong University, Jinan, Shandong, P.R. China

* Min Liu, Dapeng Zhao and Xingguo Wu contributed equally

Corresponding Author: Fengnian Rong, e-mail: fnrong@163.com

Source of support: This work was supported in part by the Key Research and Development Project of Shandong (2017G006022)

Background: Intrauterine adhesions (IUAs) are one of the most common reproductive system diseases in women worldwide. Emerging evidence has demonstrated that the upregulation or downregulation of genes plays an important role in IUAs. The aim of this study was to evaluate the role of NUS1 in IUAs in a rat model.

Material/Methods: The expression of miR-466 in intrauterine adhesions tissues was detected by using RT-qPCR assay. RT-qPCR, IHC, and Western blot were used to investigate mRNA and proteins expression, respectively, of NUS1. MTT and colony-formation assays were used to evaluate cell growth. Transwell assays were used to detect cell migration and invasion. To investigate miR-466 and NUS1 functions *in vivo*, we established a rat model. The level of epithelial-to-mesenchymal transition (EMT)-related markers was analyzed by Western blot assay.

Results: NUS1 was upregulated in IUAs tissues, and the high expression level of NUS1 was positively correlated with the severity of IUAs. NUS1 promoted cell proliferation *in vitro*. NUS1 overexpression on cell migration and invasion promoted the EMT process *in vitro* and *in vivo*. NUS1 acted as a target of miR-466 and played the stimulative role by regulating AKT/NFκB pathway.

Conclusions: Our data suggest that miR-466 and NUS1 regulate proliferation and the EMT process through the AKT/NFκB pathway in IUAs in a rat model.

MeSH Keywords: Amniotic Band Syndrome • Cell Migration Assays • Cell Proliferation • MicroRNAs

Full-text PDF: https://www.medscimonit.com/abstract/index/idArt/914202

2608 1 5 25

Indexed in: [Current Contents/Clinical Medicine] [SCI Expanded] [ISI Alerting System] [ISI Journals Master List] [Index Medicus/MEDLINE] [EMBASE/Excerpta Medica] [Chemical Abstracts/CAS]

Background

Intrauterine adhesions (IUAs), also acquainted as Asherman syndrome (AS), arise most frequently following infection or trauma [1]. It results in amenorrhea, infertility, and various complications of pregnancy, including preterm premature rupture of membranes, malpresentation, and placental abruption [2,3]. In addition, IUAs can potentially impair the blood supply to the uterus and early fetus [4,5]. These clinical symptoms are associated with major health concerns, particularly for women of childbearing age. In recent years, IUAs has become the second most common cause of female infertility due to the increasing use of uterine cavity surgery [6]. Although it is widely accepted that the disease is caused by acute inflammatory and dysregulation of transcription factors [7,8], the precise pathological mechanisms involved remain unclear.

MicroRNAs (miRNAs) are a family of small, endogenous, noncoding, single RNA molecules composed of 18–22 nucleotides (nt) that post-transcriptionally regulate gene expression by directly binding to the 3'untranslated region (UTR) of their target mRNA [9, 10]. Accumulating evidence has indicated that dysregulation of miRNAs is involved in IUAs. For example, the miR-1291 level was significantly increased in endometrium affected by IUAs. miR-1291 promoted endometrial fibrosis by regulating the ArhGAP29-RhoA/ROCK1 signaling pathway in a murine model [11]. In addition, miR-29b inhibited endometrial fibrosis by regulating the Sp1-TGF-β1/Smad-CTGF axis in a rat model [12]. miR-466 is down-regulated and functions as a suppressor gene in many diseases, including osteosarcoma [13], colorectal cancer [14], and prostate cancer [15]. However, the role and mechanism of miR-466 in IUAs are unknown.

NUS1, also known as NgBR, is a transmembrane receptor protein that has been identified as a Nogo-B-binding protein and is essential for the Nogo-B-mediated chemotaxis of endothelial cells [16]. Recently, Zhao et al. reported that NUS1 knockdown resulted in decrease of epithelial-mesenchymal transition (EMT) in MDA-MB-231 cells. Furthermore, they demonstrated that NUS1 knockdown significantly inhibited the TGF-β-induced EMT process and staining of E-cadherin protein, as well as the decreased expression of vimentin in MCF-7 cells [17]. However, the roles of NUS1 and NUS1-mediated signaling pathway in IUAs are still unclear.

In this study, we revealed that NUS1 was upregulated in IUAs tissues and the high expression of NUS1 was positively related to the severity of IUAs. In addition, we identified that NUS1 functioned as a target of miR-466 and played a stimulative role by regulating the AKT/NFκB pathway. In conclusion, our data suggest that NUS1 upregulation by miR-466 knockdown contributes to the proliferation and EMT process in IUAs through the AKT/NFκB pathway.

Table 1. Primers used for this study.

RT-qPCR primers	Primer sequence (5'-3')
miR-466-RT	GTCGTATCCAGTGCAGGGTCCGAGGT
	GCACTGGATACGACATGTGTGT
miR-466-qPCR-Fwd	TGCGGCATACACATACACGC
Oligo-dT	TTTTTTTTTTTTTTTT
U6-RT	GTCGTATCCAGTGCAGGGTCCGAGGTATTC
	GCACTGGATACGACAAAATATGGAAC
U6-Fwd	TGCGGGTGCTCGCTTCGGCAGC
miRNA-universal-Rev	CCAGTGCAGGGTCCGAGGT
NUS1-qPCR-Fwd	ACAGCGTCTGGGAAAGTA
NUS1-qPCR-Rev	AGTAGCTGGGCTGAAGAC
β-actin-qPCR-Fwd	CGTGACATTAAGGAGAAGCTG
β-actin-qPCR-Rev	CTAGAAGCATTTGCGGTGGAC

Material and Methods

Patient samples

Intrauterine adhesions and control tissues were collected between December 2017 and April 2018 from Taian City Central Hospital, Shandong, China. Twenty-five women with intrauterine adhesions were diagnosed by hysteroscopy and further confirmed by pathology. The r-AFS intrauterine adhesion score standard was used for disease stage (8 were mild stage, 10 were moderate stage, and 7 were severe stage). Endometrial tissues were obtained by scraping the endometrium with a uterine curette during hysteroscopic procedure from the adhesion sites of IUA and the control patients. Cases selected were all women of reproductive age (women aged ≤40 years). Twenty-five normal endometrial tissues from patients without IUA and uterine septum who received hysteroscopy due to male infertility or other factors in the same period were used as controls. Written informed consent was obtained from all patients, and the study protocols were approved by the Institutional Ethics Committee of Taian City Central Hospital.

RT-qPCR assay

Total RNAs were extracted using TRIzol reagent (Invitrogen Inc., Carlsbad, CA, USA) and the reverse transcription reactions were performed using an RT Kit (Qiagen GmbH, Hilden, Germany). Relative mRNAs and miR-466 levels were evaluated by real-time quantitative PCR with SYBR Green Master mix (Applied Biosystems; Thermo Fisher Scientific, Inc.) using a Biosystems7500 (Invitrogen; Thermo Fisher Scientific, Inc.). The PCR conditions consisted of 4 min at 94°C for 1 cycle,

Indexed in: [Current Contents/Clinical Medicine] [SCI Expanded] [ISI Alerting System] [ISI Journals Master List] [Index Medicus/MEDLINE] [EMBASE/Excerpta Medica] [Chemical Abstracts/CAS]

followed by 33 cycles of 94°C for 30 s, 58°C for 30 s, and 72°C for 30 s. The primer sequences are shown in Table 1.

Cell culture and transfection

Cells were grown in 1640 medium (Gibco, Waltham, MA) supplemented with 10% FBS (Gibco, Waltham, MA) and 1% penicillin/streptomycin in a 5% CO_2 atmosphere at 37°C. Cells were seeded into plates 1 day before and transfected with the indicated plasmids using Lipofectamine 2000 (Invitrogen; Thermo Fisher Scientific, Inc.) following the manufacturer's instructions.

IHC staining

IHC was performed as previously described using anti-NUS1 antibody (1: 200; Abcam, Cambridge, MA, USA) [18]. HE staining was performed as previously described [19]. For HE staining, the slides were first deparaffinized and rehydrated, and then stained with hematoxylin and eosin (HE).

Uterine inflammation rat model

This study was carried out in strict accordance with the recommendations of the Guide for the Care and Use of Laboratory Animals of the National Institutes of Health. The protocol was approved by the Ethics Committee of Taian City Central Hospital. Female rats weighting 260–280 g were purchased from CAMS (Chinese Academy of Medical Sciences, Shanghai, China). The model was performed as previously described [7].

Bioinformatics prediction for target genes

The target genes of miR-466 were predicted using online software, including miRNA.org and TargetScan 7.1.

EGFP reporter assay

Cells were seeded in 48-well plates 1 day before transfection, and then co-transfected with pri-miR-466 or Anti-miR-466 and pEGFP-NUS1 3'UTR, pEGFP-NUS13'UTR mut. The vector pDsRed2-N1 (Clontech, 632406), which expresses RFP, was included for transfection normalization. After transfection for 48 h, the cells were lysed using radio-immunoprecipitation assay (RIPA) lysis buffer (Sigma, R0278), and the EGFP and RFP intensities were measured with a fluorescence spectrophotometer (Hitachi, F4500).

MTT assay

H8 and End1/E6E7 cells were seeded in 96-well plates at 5000 cells per well 1 day prior to transfection. Cell viability was determined by MTT assay. Then, 10 µl of 5mg/ml MTT (Sigma, 298931) was added and incubated for 6 h. The medium was aspirated and MTT was dissolved in 100 µl DMSO (Sigma, 67685) and absorbance was read at 570 nm using a Quant Universal microplate spectrophotometer.

Transwell migration and invasion assay

Cell migration and invasion ability was evaluated by a Transwell assay, as described previously. Briefly, 6×10^5 H8 and End1/E6E7 cells in 200 µl of serum-free medium were cultured in a chamber containing an 8-µm polycarbonate filter (Millipore, USA) coated with 30 µl of Matrigel (BD) for the invasion assay. After incubating for 48 h, cells remaining on the upper membrane were removed with a cotton swab and cells that had penetrated the membrane were fixed with 4% formaldehyde and then stained with 0.5% crystal violet for 30 min. The cells were then photographed and quantified in 5 random fields.

Immunofluorescence staining (IF)

Cells transfected with the indicated plasmids before IF assay. Forty-eight hours later, the cells were washed with 1×PBS, fixed in 4% paraformaldehyde for 30 min and blocked with 10% donkey serum (Beyotime Institute of Biotechnology; Nanjing, China) for 30 min at room temperature. The primary antibody against p65 was incubated overnight at 4°C. The fluorescein isothiocyanate (FITC)-conjugated secondary antibody was added and incubated for 2 h, followed by incubation with DAPI. Fluorescence images were captured using a confocal microscope.

Western blot analysis

Cells and tissues were lysed using the Protein Extraction kit (Wanlei Biotechnology, Beijing, China). The proteins were separated by SDS-polyacrylamide gel electrophoresis and transferred to polyvinylidene difluoride (PDVF) membranes. The membranes were blocked with skimmed milk (5%, w/v). The membranes were probed with anti-E-cadherin (1: 2000; Abcam, Cambridge, MA, USA), anti-Vimentin (1: 3000; Abcam, Cambridge, MA, USA), anti-NUS1 (1: 2000; Abcam, Cambridge, MA, USA), p-AKT (1: 5000; Abcam), total-AKT (1: 2000; Abcam), p-IKKα (1: 2000; Abcam), total-IKKα (1: 2000; Abcam), total-p65 (1: 3000; Abcam), p-p65 (1: 2000; Abcam), and anti-GAPDH (1: 3000; Abcam) antibodies overnight at 4˚C. The membranes were washed with TBST and incubated with horseradish peroxidase-conjugated secondary antibody for 2 h and the immunocomplexes were then visualized using a New Super ECL Detection Kit (KeyGEN BioTECH, China) according to the manufacturer's protocol.

Statistical analysis

All analyses were performed using GraphPad Prism 5.0. Continuous data are presented as the means of 3 independent

Indexed in: [Current Contents/Clinical Medicine] [SCI Expanded] [ISI Alerting System] [ISI Journals Master List] [Index Medicus/MEDLINE] [EMBASE/Excerpta Medica] [Chemical Abstracts/CAS]

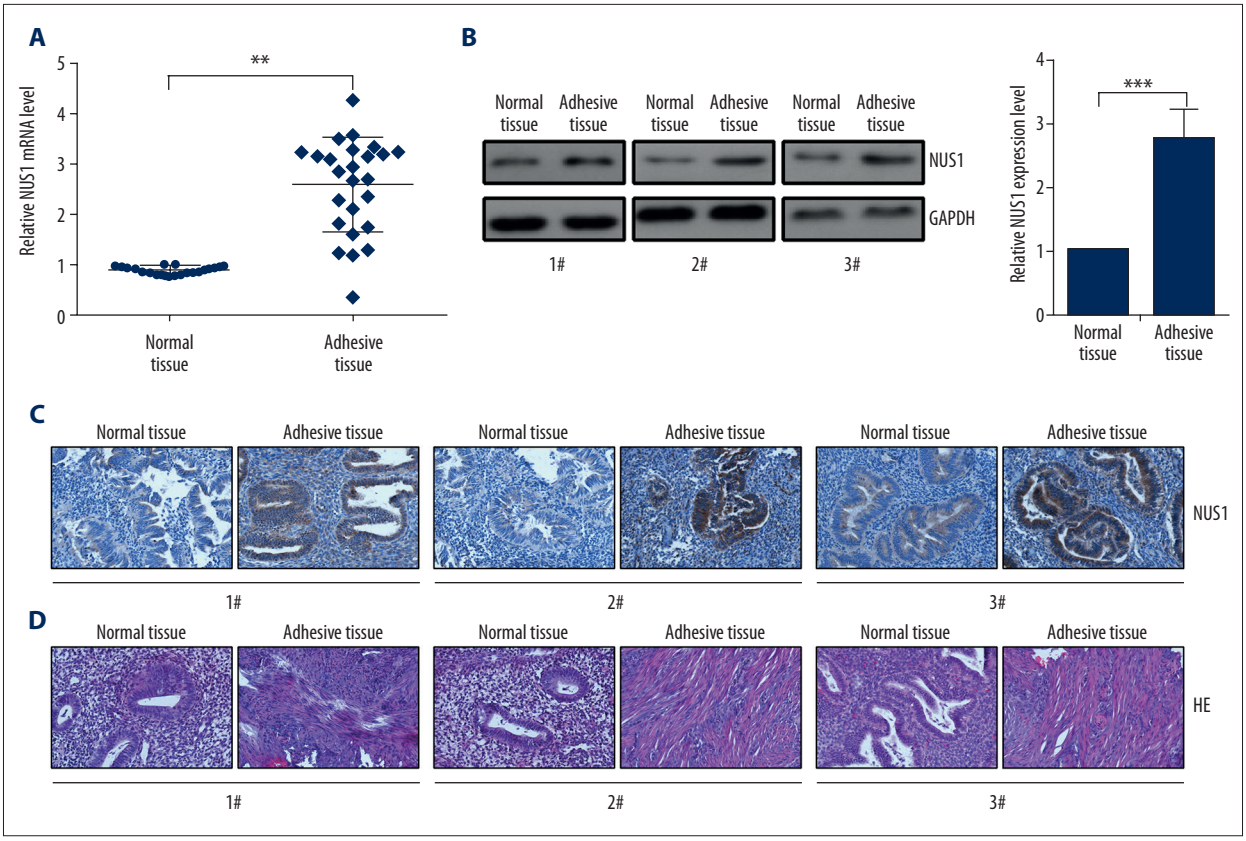

Figure 1. NUS1 was upregulated in IUAs tissues. (**A**) The mRNA levels of NUS1 in normal tissues and IUAs (n=25) tissues were evaluated by RT-qPCR assay. (**B**) Protein levels of NUS1 in normal tissues and IUAs (n=25) tissues were evaluated by Western blot assay. (**C**) The expression of NUS1 in normal tissues and IUAs (n=25) tissues were evaluated by IHC staining. (**D**) HE staining showed the abnormal morphology in IUAs tissues. Results are presented as the mean ±S.D from 3 independent experiments. ** P<0.01, and *** P<0.001.

experiments ± standard error of the mean, and analyzed using the *t* test. Differences were considered statistically significant at two-sided P<0.05.

Results

NUS1 expression was upregulated in IUAs tissues

To examine the levels of NUS1 in IUAs, RT-qPCR assay was performed. The results indicated a significant increase in the expression of NUS1 in 25 pairs of IUAs tissues compared with the adjacent non-IUAs tissues (Figure 1A). In addition, Western blot assay showed that an increasing expression of NUS1 protein in IUAs tissues than that in the adjacent non-IUAs tissues (Figure 1B). We performed IHC staining to determine NUS1 protein level and location in IUAs patient and the normal control samples. Our IHC data revealed that the NUS1 protein expression in the IUAs samples was strongly expressed and mainly located in the cytoplasm (Figure 1C). As shown in Figure 1D, HE staining of the uteruses revealed abnormal morphology in the IUAs group. The endometrial structure was irregular, with increased numbers of fibroblasts (Figure 1D).

NUS1 overexpression promoted cell proliferation and EMT process

To explore the molecular mechanism of NUS1 in IUAs, loss-of-function or gain-of-function assays were performed to identify whether NUS1 can regulate cervical cell phenotype in H8 and End1/E6E7 cells (Figure 2A, 2B). MTT assay revealed that ectopically expressing NUS1 in H8 and End1/E6E7 cells markedly enhanced their viability, and shR-NUS1 transfection inhibited cell viability in H8 and End1/E6E7 cells (Figure 2C). Colony formation assay showed that NUS1 overexpression in H8 and End1/E6E7 cells resulted in a significant increase in cell proliferation, and knockdown of NUS1 in H8 and End1/E6E7 cells inhibited cell proliferation (Figure 2D). Flow cytometry assay showed a significant decrease in the percentage of cells in G1 phase and an increase in the percentage of cells in S and G2 phases in H8 and End1/E6E7 cells transfected with the pNUS1. We also found a decrease in the percentage of cells in

Indexed in: [Current Contents/Clinical Medicine] [SCI Expanded] [ISI Alerting System] [ISI Journals Master List] [Index Medicus/MEDLINE] [EMBASE/Excerpta Medica] [Chemical Abstracts/CAS]

G1 phase and an increase in the percentage of cells in S and G2 phase in H8 and End1/E6E7 cells transfected with shR-NUS1 (Figure 2E). Apoptosis assay showed that NUS1 overexpression decreased the percentage of apoptotic cells in H8 and End1/E6E7 cells, while inhibition of NUS1 caused a significant increase the percentage of apoptotic cells in H8 and End1/E6E7 cells (Figure 2F). Transwell migration and invasion assays showed the increased migration and invasion abilities after NUS1 overexpression in H8 and End1/E6E7 cells, and we found decreased migration and invasion abilities by knockdown of NUS1 in H8 and End1/E6E7 cells (Figure 2G, 2H). As shown in Figure 2I, the epithelial cell marker E-cadherin was significantly decreased, while the mesenchymal cell marker vimentin was significantly increased by NUS1 overexpression, and the opposite effects were observed in the inhibition of NUS1 in H8 and End1/E6E7 cells (Figure 2I).

NUS1 was directly targeted by miR-466

We performed bioinformatics analysis to predict the targeted miRNAs on NUS1 using microRNA.org and TargetScan (Figure 3A). We first constructed the 3'UTR and 3'UTR mut reporter vectors of NUS1, as indicated in Figure 3B (Figure 3B). Then, we constructed the overexpression and knockdown vectors of miR-466 and validated its efficiencies in H8 and End1/E6E7 cells (Figure 3C). Co-transfection with miR-466 and the NUS1 3'UTR reporter significantly decreased EGFP intensities, while we found increased EGFP intensities by co-transfection with ASO-miR-466 and the NUS1 3'UTR reporter. However, after co-transfection pri-miR-466 or ASO-miR-466 with the mutated 3'UTR reporter, the EGFP intensities were unchanged (Figure 3D, 3E). As shown in Figure 3F and 3G, the mRNA and protein levels of NUS1 were significantly reduced by transfection miR-466 expression vector compared with the empty vector control in H8 and End1/E6E7 cells (Figure 3F, 3G).

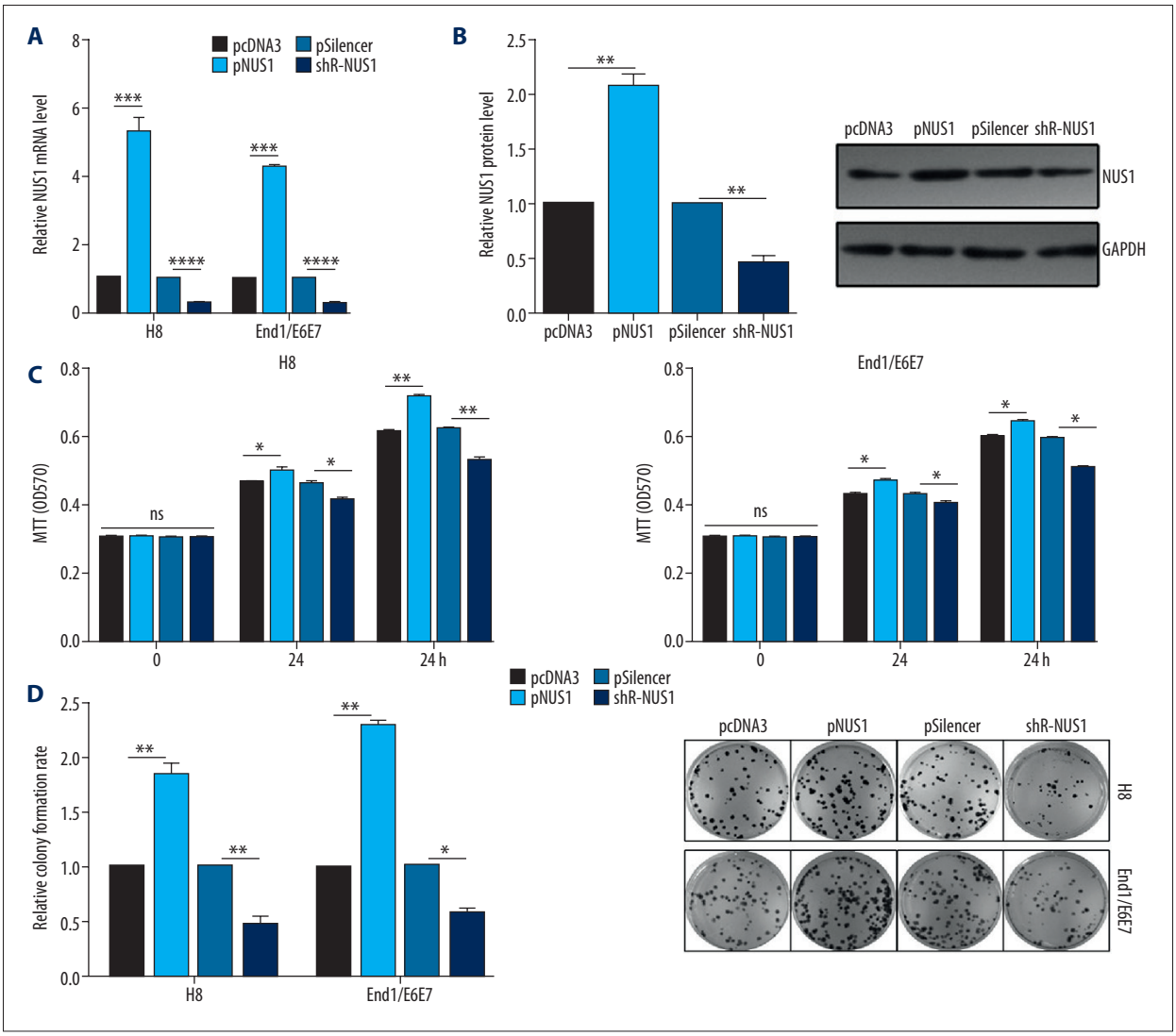

Indexed in: [Current Contents/Clinical Medicine] [SCI Expanded] [ISI Alerting System] [ISI Journals Master List] [Index Medicus/MEDLINE] [EMBASE/Excerpta Medica] [Chemical Abstracts/CAS]

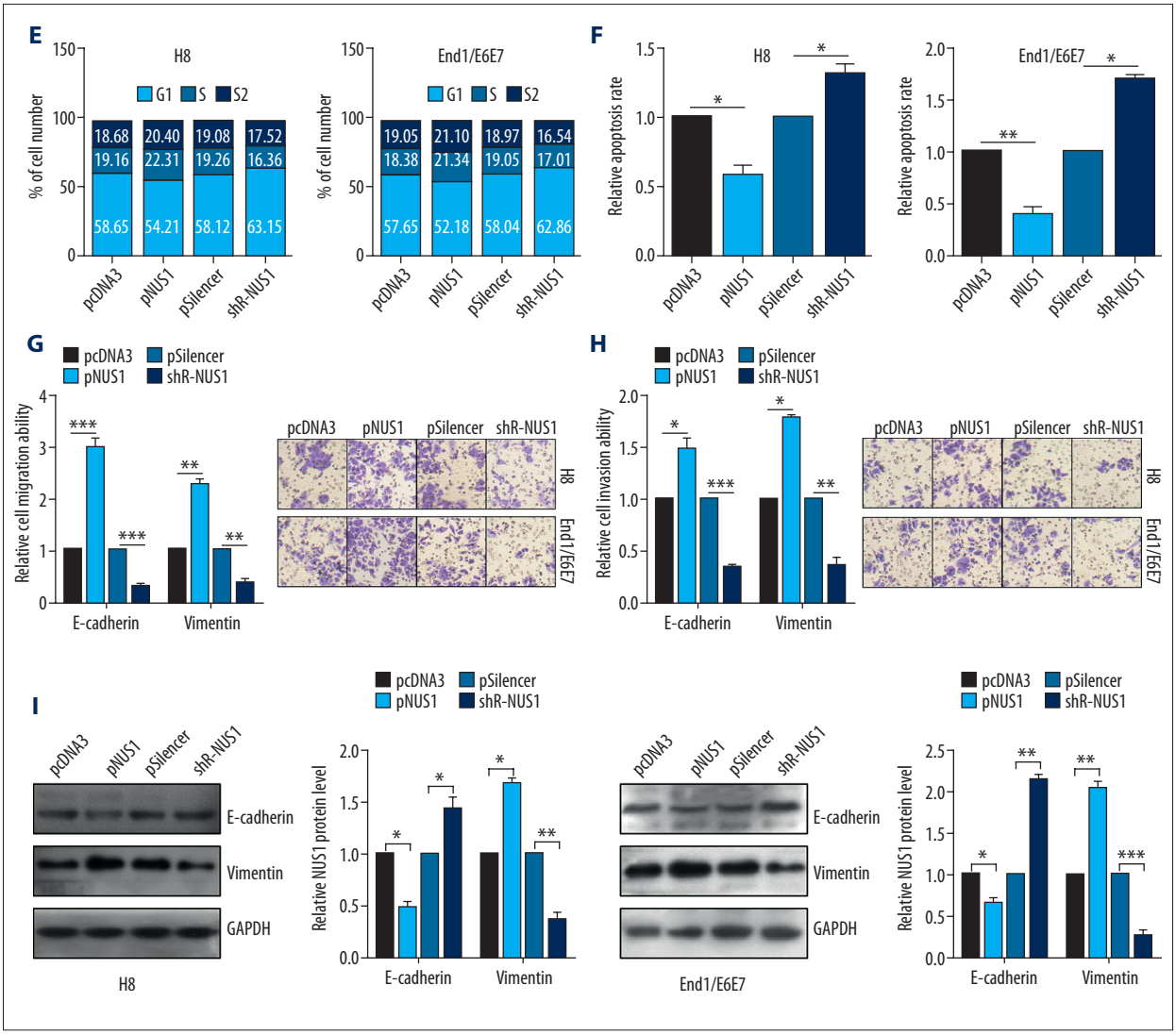

Figure 2. NUS1 promoted cell proliferation and EMT process. (**A**) Confirmation of the effectiveness of pNUS1 and shR-NUS1 by RT-qPCR in H8 and End1/E6E7 cells. (**B**) MTT assay showed the effects of NUS1 on cell viability in H8 and End1/E6E7 cells. (**C**) Colony formation assays in H8 and End1/E6E7 cells treated with pNUS1 or shR-NUS1 and the control group. (**D**) The cell cycle of H8 and End1/E6E7 cells transfected with pcDNA3 or pNUS1 or pSilencer or shR-NUS1 was detected by flow cytometry. (**E, F**) Apoptosis rates of H8 and End1/E6E7 cells treated with pcDNA3 or pNUS1 or pSilencer or shR-NUS1 were detected by flow cytometry. (**G, H**) Transwell assay was used to detect the cell migration and invasion ability. (**I**) Western blot assay showed the protein levels of E-cadherin and Vimentin after transfection with the indicated plasmids in H8 and End1/E6E7 cells. Results are presented as the mean ± S.D from 3 independent experiments. *P<0.05, **P<0.01, and ***P<0.001.

miR-466 inhibited cell proliferation and EMT process *in vitro* and *in vivo* by regulating NUS1

MTT analysis and colony formation analysis showed that miR-466 inhibited the cell growth in H8 and End1/E6E7 cells, presented as decreased MTT OD570 value and decreased colony formation rate, respectively. However, NUS1 overexpression reversed the decreased growth effects induced by miR-466 (Figure 4A, 4B). Transwell assay showed that miR-466 inhibited cell migration and invasion in H8 and End1/E6E7 cells. In contrast, after co-transfection with pri-miR-466 and NUS1, the migration and invasion abilities were neutralized by the addition of miR-466 in H8 and End1/E6E7 cells (Figure 4C, 4D). To provide direct evidence of the role of miR-466 and NUS1 in regulating pathogenesis of IUAs, we established an intrauterine adhesion rat model using LPS, as detailed previously [7]. As shown in Figure 4E, IHC staining of the uteruses revealed the low expression of NUS1 in the miR-466-treated group compared with the control group in the modeling IUAs. Co-treatment with pri-miR-466 and NUS1 neutralized the NUS1 expression

Indexed in: [Current Contents/Clinical Medicine] [SCI Expanded] [ISI Alerting System] [ISI Journals Master List] [Index Medicus/MEDLINE] [EMBASE/Excerpta Medica] [Chemical Abstracts/CAS]

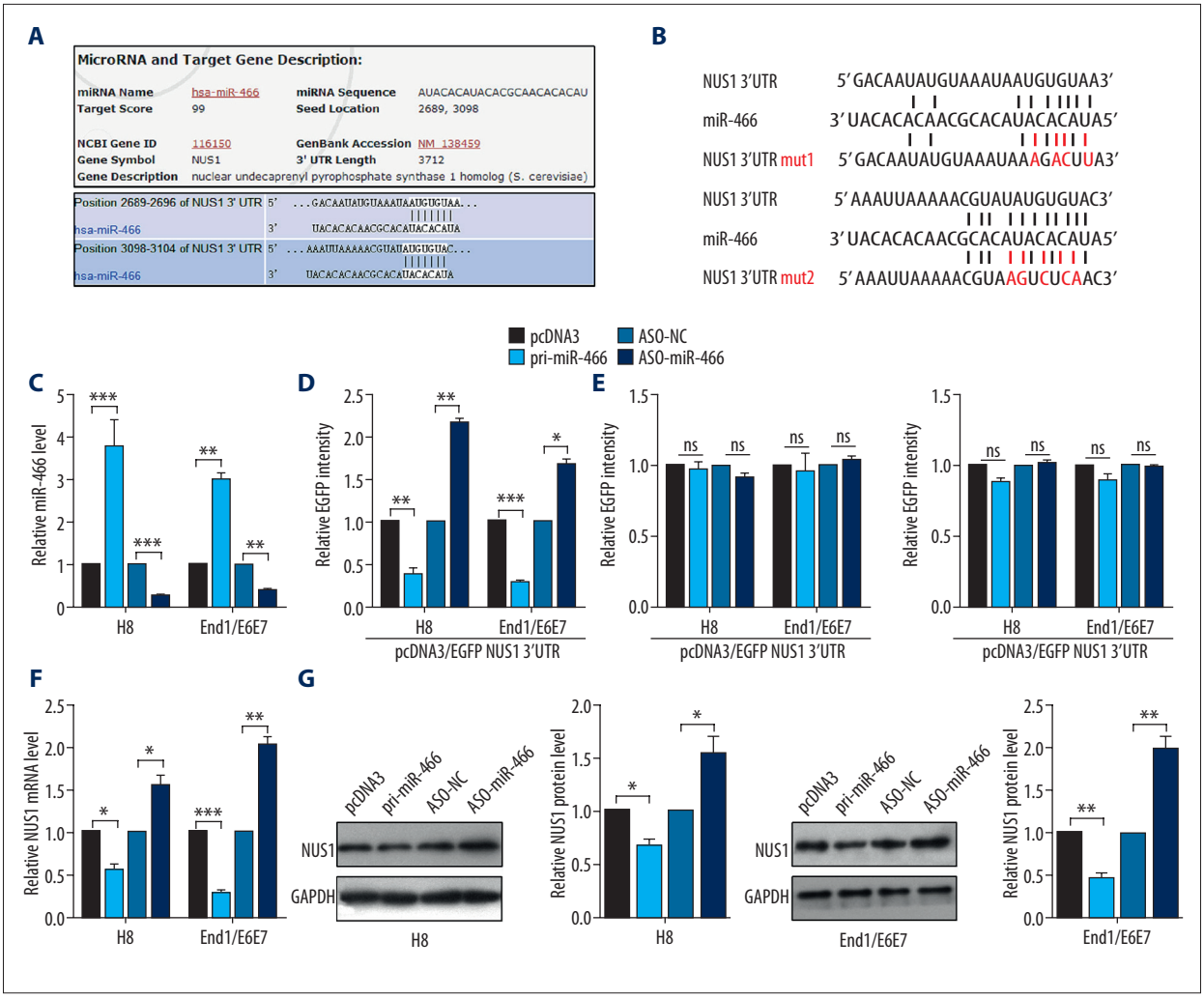

Figure 3. miR-466 directly targeted NUS1. (**A, B**) Predicted miR-466 target sequences in the 3'UTR of NUS1 and the mutant containing altered nucleotides in the 3'UTR of NUS1. (**C**) Confirmation of the effectiveness of pri-miR-466 and ASO-miR-466 by RT-qPCR in H8 and End1/E6E7 cells. (**D**) EGFP assay of the indicated cells transfected with pcDNA3/EGFP-NUS13'UTR reporters and the indicated plasmids. (**E**) EGFP assay of H8 and End1/E6E7 cells transfected with pcDNA3/EGFP-NUS1 3'UTR mut reporters and the indicated plasmids. (**F**) Confirmation of the NUS1 mRNA level transfected with the indicated plasmids by RT-qPCR assay. (**G**) Confirmation of the relative protein expression levels of NUS1transfected with the indicated plasmids by Western blot assay. Results are presented as the mean ±S.D from 3 independent experiments. * P<0.05, ** P<0.01, and *** P<0.001.

(but this was not found in the miR-466-treated group) in the modeling IUAs (Figure 4E). We performed Western blot assay and found that the modeling IUAs from the miR-466 group had increased E-cadherin expression and decreased vimentin expression compared with the control group (Figure 4F).

miR-466 inhibited the AKT/NFκB pathway through NUS1

To determine whether miR-466 regulates the AKT/NFκB signaling pathway, the expression levels of AKT/NFκB-associated genes and the activity of NFκB were analyzed. We found that miR-466 inactivated the AKT/NF-κB pathway, as indicated by the inhibited expressions of the phosphorylated form of AKT, IKKα, and p65, but with no changes in the total expressions of AKT, IKKα, and p65 (Figure 5A). In addition, IF assay showed that the nuclear distribution of p65 in End1/E6E7 cell was decreased in pri-miR-466-transfected cells and rescued by pNUS1 transfection in miR-466-overexpressing cells (Figure 5B). Reporter analyses showed significantly decreased NFκB luciferase activities after miR-466 treatment, but not after treatment with the combination of miR-466 and NUS1 in End1/E6E7 cells (Figure 5C).

Indexed in: [Current Contents/Clinical Medicine] [SCI Expanded] [ISI Alerting System] [ISI Journals Master List] [Index Medicus/MEDLINE] [EMBASE/Excerpta Medica] [Chemical Abstracts/CAS]

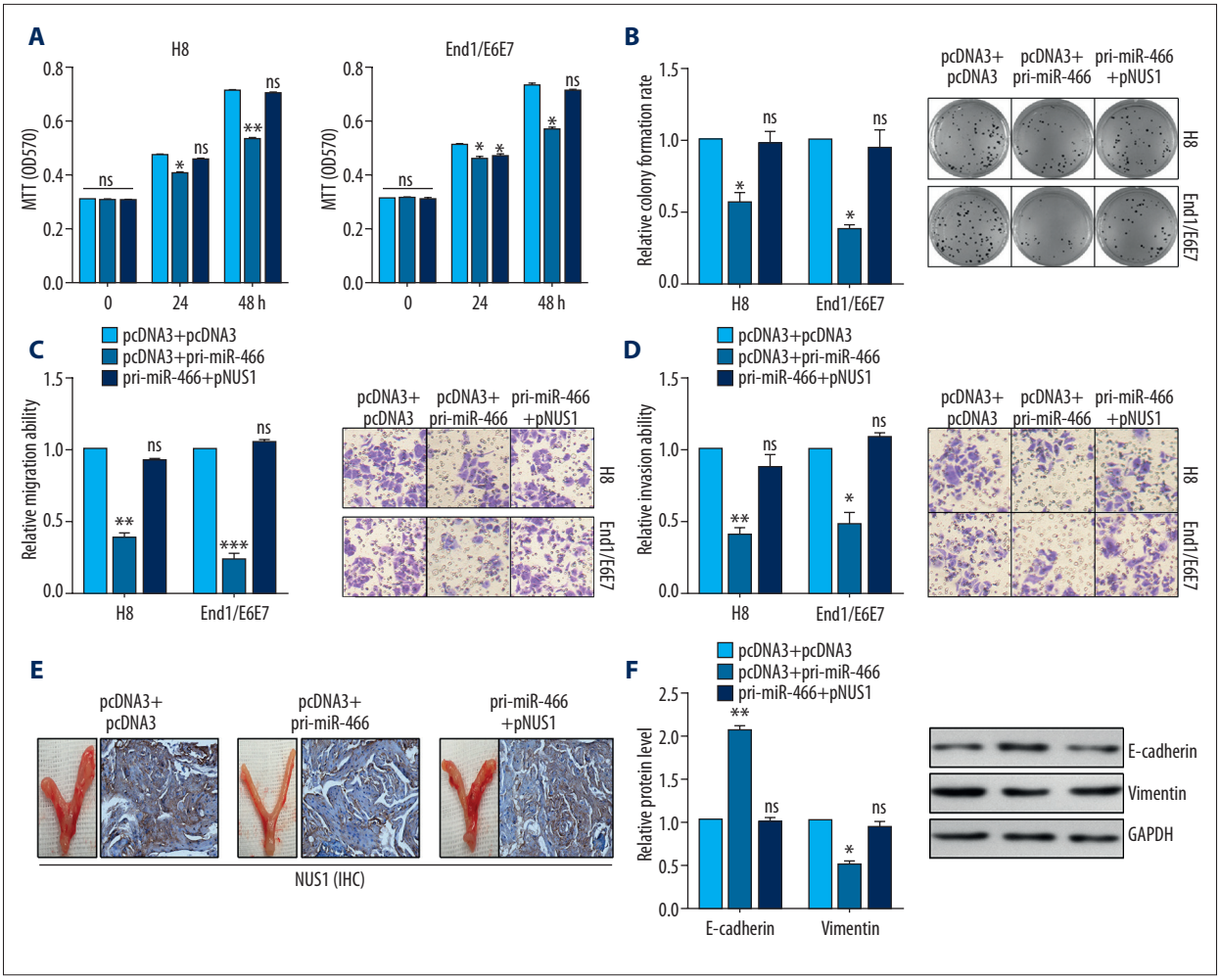

Figure 4. miR-466 inhibited cell proliferation and EMT process by regulating NUS1. (**A**) MTT assay showed the effects of the indicated transfection on cell viability in H8 and End1/E6E7 cells. (**B**) Colony formation assays in H8 and End1/E6E7 cells treated with the indicated plasmids showed the cell proliferation. (**C, D**) Transwell assay was used to detect the cell migration and invasion ability transfected with the indicated plasmids in H8 and End1/E6E7 cells. (**E**) IHC staining showed the expression of NUS1 in IUAs model of rat tissues treated with the indicated plasmids. (**F**) Western blot assay showed the expression of E-cadherin and Vimentin in IUAs model of rat tissues treated with the indicated plasmids. Results are presented as the mean ±S.D from 3 independent experiments. * P<0.05, ** P<0.01, and *** P<0.001.

Discussion

IUAs is one of the most common reproductive system diseases in women worldwide [20]. Understanding the causes and related molecular mechanisms of intrauterine adhesions is essential for the prevention and treatment of Asherman syndrome. Emerging evidence has demonstrated that the upregulation or downregulation of genes plays an important role in IUAs. For example, Xiao et al. reported that the expression of SOX2, NANOG, and OCT4 was upregulated in a mouse model of LPS-induced acute uterine injury [7]. In addition, the upregulation of CXCL12 promoted stem cell recruitment and uterine repair after injury in IUAs [8]. Salma et al. also suggested that TGF-β1/Smad3/smad7 was a major pathway which plays an important role in the regulation of the IUAs, and specific inhibitor of Smad3 (SIS3) may provide a new therapeutic strategy for IUAs [21]. In the present study, we found that NUS1 was upregulated in IUAs patients. Upregulation of NUS1 promoted cell proliferation, migration, and invasion *in vitro* and *in vivo*, accelerated the cell cycle process, and inhibited cell apoptosis in H8 and End1/E6E7 cells. Furthermore, we found that NUS1 was directly targeted by miR-466 in H8 and End1/E6E7 cells.

Recently, Dong et al. reported that NUS1 activated the AKT pathway and thus increased the resistance of human hepatocellular cancer cells to 5-FU [22]. Wang et al. reported that NFκB is a novel pathogenesis factor of Asherman syndrome and provided new insights into the prevention and treatment

Indexed in: [Current Contents/Clinical Medicine] [SCI Expanded] [ISI Alerting System] [ISI Journals Master List] [Index Medicus/MEDLINE] [EMBASE/Excerpta Medica] [Chemical Abstracts/CAS]

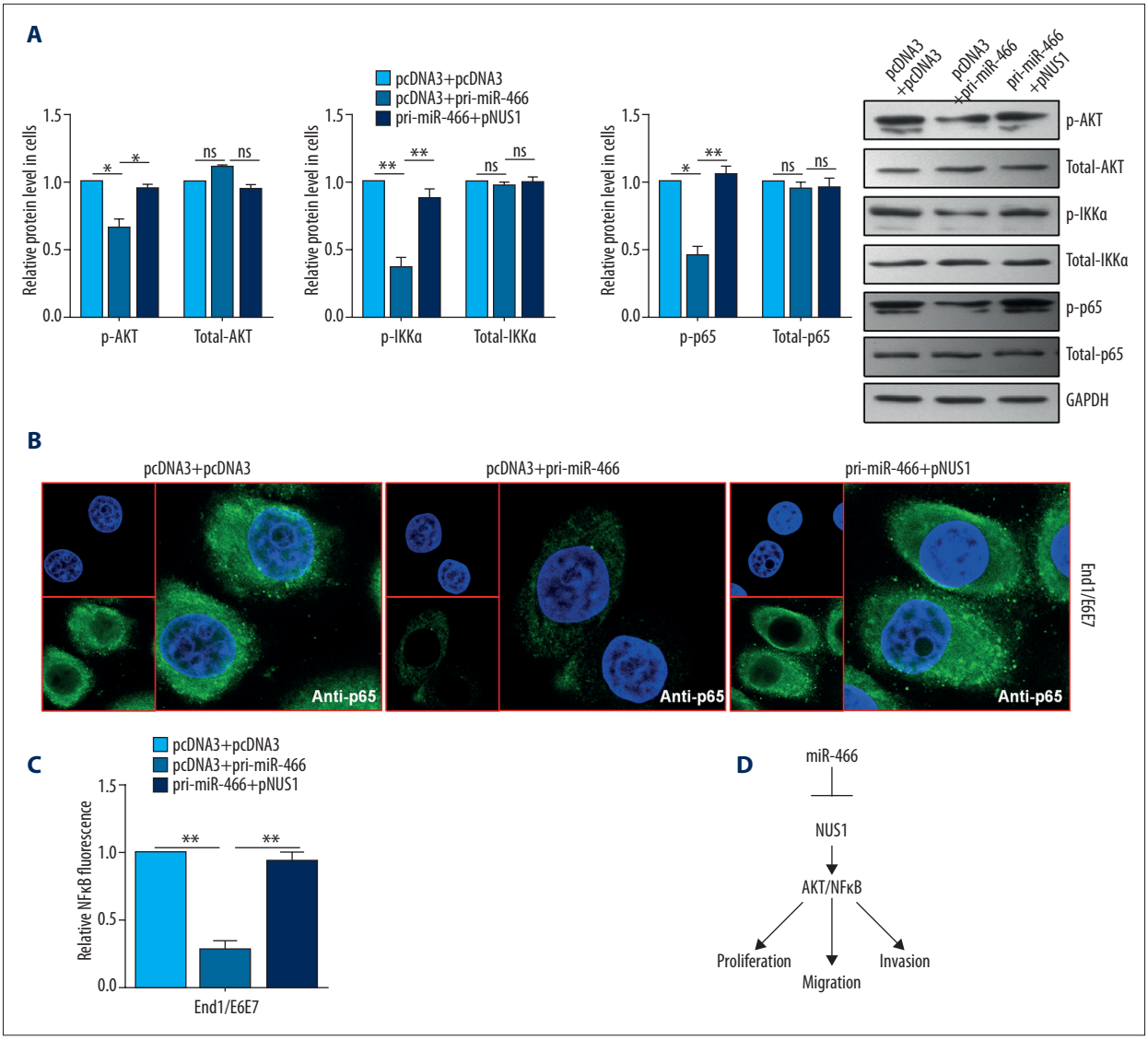

Figure 5. miR-466 inhibited the AKT/NFκB pathway through NUS1. (**A**) Western blot analysis was conducted to detect the expression levels of p-AKT, total-AKT, p-IKKα, total-IKKα, p-p65, and total-p65 in End1/E6E7 cells. (**B**) Immunofluorescence staining was used to examine the nuclear distribution of p65 in End1/E6E7 cells. (**C**) Relative NFκB luciferase ratio was detected with the indicated plasmids in End1/E6E7 cells. (**D**) The model of miR-466 and NUS1 regulation relationship. Results are presented as the mean ±S.D from 3 independent experiments. * P<0.05, ** P<0.01, and *** P<0.001.

of intrauterine adhesions in Asherman syndrome patients [23]. The NFκB transcription factor promotes the expression of intrauterine adhesion inflammatory factors and plays a central role in inflammatory diseases [24,25]. In this study, we found that miR-466 inactivates AKT/NFκB pathway by regulating NUS1 in H8 and End1/E6E7 cells and then affects the IUAs process.

Conclusions

The present study results establish that miR-466 acts upstream of NUS1 to negatively regulate the AKT/NFκB pathway, ultimately inhibiting IUAs (Figure 5D). These results elucidate the mechanism involved in formation of IUAs and may provide new potential therapeutic options for patients with IUAs.

Conflicts of interest

None.

Indexed in: [Current Contents/Clinical Medicine] [SCI Expanded] [ISI Alerting System] [ISI Journals Master List] [Index Medicus/MEDLINE] [EMBASE/Excerpta Medica] [Chemical Abstracts/CAS]

References:

1. Buttram VC Jr., Turati G: Uterine synechiae: variations in severity and some conditions which may be conducive to severe adhesions. Int J Fertil, 1977; 22(2): 98–103
2. Tuuli MG, Shanks A, Bernhard L et al: Uterine synechiae and pregnancy complications. Obstet Gynecol, 2012; 119(4): 810–14
3. Lin N, Li X, Song T et al: The effect of collagen-binding vascular endothelial growth factor on the remodeling of scarred rat uterus following full-thickness injury. Biomaterials, 2012; 33(6): 1801–7
4. Carp HJ, Ben-Shlomo I, Mashiach S: What is the minimal uterine cavity needed for a normal pregnancy? An extreme case of Asherman syndrome. Fertil Steril, 1992; 58(2): 419–21
5. Taylor PJ, Cumming DC, Hill PJ: Significance of intrauterine adhesions detected hysteroscopically in eumenorrheic infertile women and role of antecedent curettage in their formation. Am J Obstet Gynecol, 1981; 139(3): 239–42
6. Roge P, Cravello L, D'Ercole C et al: Intrauterine adhesions and fertility: Results of hysteroscopic treatment. Gynaecological Endoscopy, 1997; 6(4): 225–28
7. Xiao L, Song Y, Huang W et al: Expression of SOX2, NANOG and OCT4 in a mouse model of lipopolysaccharide-induced acute uterine injury and intrauterine adhesions. Reprod Biol Endocrinol, 2017; 15(1): 14
8. Sahin Ersoy G, Zolbin MM, Cosar E et al: CXCL12 promotes stem cell recruitment and uterine repair after injury in Asherman's syndrome. Mol Ther Methods Clin Dev, 2017; 4: 169–77
9. He L, Hannon GJ: MicroRNAs: Small RNAs with a big role in gene regulation. Nat Rev Genet, 2004; 5(7): 522–31
10. Bartel DP: MicroRNAs: Genomics, biogenesis, mechanism, and function. Cell, 2004; 116(2): 281–97
11. Xu Q, Duan H, Gan L et al: MicroRNA-1291 promotes endometrial fibrosis by regulating the ArhGAP29-RhoA/ROCK1 signaling pathway in a murine model. Mol Med Rep, 2017; 16(4): 4501–10
12. Li J, Du S, Sheng X et al: MicroRNA-29b inhibits endometrial fibrosis by regulating the Sp1-TGF-beta1/Smad-CTGF axis in a rat model. Reprod Sci, 2016; 23(3): 386–94
13. Cao W, Fang L, Teng S et al: MicroRNA-466 inhibits osteosarcoma cell proliferation and induces apoptosis by targeting CCND1. Exp Ther Med, 2018; 16(6): 5117–22
14. Tong F, Ying Y, Pan H et al: MicroRNA-466 (miR-466) functions as a tumor suppressor and prognostic factor in colorectal cancer (CRC). Bosn J Basic Med Sci, 2018; 18(3): 252–59
15. Colden M, Dar AA, Saini S et al: MicroRNA-466 inhibits tumor growth and bone metastasis in prostate cancer by direct regulation of osteogenic transcription factor RUNX2. Cell Death Dis, 2017; 8(1): e2572
16. Miao RQ, Gao Y, Harrison KD et al: Identification of a receptor necessary for Nogo-B stimulated chemotaxis and morphogenesis of endothelial cells. Proc Natl Acad Sci USA, 2006; 103(29): 10997–1002
17. Zhao B, Xu B, Hu W et al: Comprehensive proteome quantification reveals NgBR as a new regulator for epithelial-mesenchymal transition of breast tumor cells. J Proteomics, 2015; 112: 38–52
18. Liang Y, Zhu F, Zhang H et al: Conditional ablation of TGF-beta signaling inhibits tumor progression and invasion in an induced mouse bladder cancer model. Sci Rep, 2016; 6: 29479
19. Lin S, Shen H, Jin B et al: Brief report: Blockade of Notch signaling in muscle stem cells causes muscular dystrophic phenotype and impaired muscle regeneration. Stem Cells, 2013; 31(4): 823–28
20. Johary J, Xue M, Zhu X et al: Efficacy of estrogen therapy in patients with intrauterine adhesions: Systematic review. J Minim Invasive Gynecol, 2014; 21(1): 44–54
21. Salma U, Xue M, Ali Sheikh MS et al: Role of transforming growth factor-beta1 and Smads signaling pathway in intrauterine adhesion. Mediators Inflamm, 2016; 2016: 4158287
22. Dong C, Zhao B, Long F et al: Nogo-B receptor promotes the chemoresistance of human hepatocellular carcinoma via the ubiquitination of p53 protein. Oncotarget, 2016; 7(8): 8850–65
23. Wang X, Ma N, Sun Q et al: Elevated NF-kappaB signaling in Asherman syndrome patients and animal models. Oncotarget, 2017; 8(9): 15399–406
24. Yimam M, Lee YC, Moore B et al: Analgesic and anti-inflammatory effects of UP1304, a botanical composite containing standardized extracts of *Curcuma longa* and *Morus alba*. J Integr Med, 2016; 14(1): 60–68
25. Lawrence T: The nuclear factor NF-kappaB pathway in inflammation. Cold Spring Harb Perspect Biol, 2009; 1(6): a001651

Indexed in: [Current Contents/Clinical Medicine] [SCI Expanded] [ISI Alerting System] [ISI Journals Master List] [Index Medicus/MEDLINE] [EMBASE/Excerpta Medica] [Chemical Abstracts/CAS]